Optical properties of cubic GaN from 1 to 20 eV

Martin Feneberg*
Institut für Experimentelle Physik, Otto-von-Guericke-Universität Magdeburg, Universitätsplatz 2, 39106 Magdeburg, Germany

Marcus Röppischer, Christoph Cobet, and Norbert Esser
Leibniz-Institut für Analytische Wissenschaften - ISAS - e.V., Albert-Einstein-Strasse 9, 12489 Berlin, Germany

Jörg Schörmann,† Thorsten Schupp, and Donat J. As
Department of Physics, University of Paderborn, Warburger Strasse 100, 33098 Paderborn, Germany

Florian Hörich, Jürgen Bläsing, Alois Krost, and Rüdiger Goldhahn
Institut für Experimentelle Physik, Otto-von-Guericke-Universität Magdeburg, Universitätsplatz 2, 39106 Magdeburg, Germany
(Received 15 February 2012; revised manuscript received 12 April 2012; published 26 April 2012)

We present a comprehensive overview of the optical properties of zinc-blende GaN. By a variety of different methods, such as temperature-dependent photoluminescence, photoluminescence excitation spectroscopy, photoreflectance, and ellipsometry, we investigate its emission and absorption related characteristics. The sample under study is a nearly strain-free epitaxial layer grown on freestanding cubic SiC. The light-hole/heavy-hole exciton was found at 3.271 eV at 5 K, shifting to 3.208 eV at 295 K. The split-off exciton transition was detected to be 21 meV higher in energy. Taking the difference in the exciton binding energies into account, this yields a spin-orbit energy of $\Delta_{so} = 15$ meV. Donor and acceptor binding energies could be estimated by photoluminescence to be 30 and 130 meV, respectively. By synchrotron-based spectroscopic ellipsometry the complex dielectric function up to an energy of 20 eV could be determined. Comparison with *ab initio* calculations allows an assignment of high-energy features to the peculiarities of the band structure.

DOI: 10.1103/PhysRevB.85.155207 PACS number(s): 71.35.−y, 77.22.Ch

I. INTRODUCTION

There is an ongoing interest in growth and characterization of (001)-oriented group-III nitride semiconductors with nonpolar zinc-blende crystal structure.[1,2] In comparison to the widely used wurtzite heterostructures with (0001) orientation, built-in electric fields caused by gradients of the spontaneous and piezoelectric polarization[3] are absent. The redshift of the near-infrared intersubband transitions of GaN/Al(Ga)N superlattices,[4,5] the analysis of interband transitions of Al(Ga)N/GaN quantum wells,[2,6] or the exciton spin polarization for GaN/AlN quantum dots[7] confirmed that no built-in fields cause a quantum confined Stark effect in cubic low-dimensional heterostructures. Moreover, reproducible negative differential resistance has been demonstrated for zinc-blende AlGaN/GaN double-barrier tunnel devices.[8] The high p-type conductivity in (Ga,Mn)N films[9] represents another very promising property of zinc-blende materials, opening the possibility to achieve ferromagnetism in semiconductors above room temperature (RT).

Although cubic GaN (c-GaN) is nowadays used as active material in heterostructures, its band structure and optical properties are not well known yet. Most studies of films grown on different substrates focused on the behavior around the band gap only.[10–12] For example, temperature-dependent photoreflectance (PR) studies of c-GaN layers deposited on 3μm-thick 3C-SiC/Si(001) and GaAs yielded two well-resolved excitonic absorption features for which the transition energy of the low-energy one at RT amounted to 3.195 (Ref. 10) and 3.205 eV (Ref. 11), respectively. The difference in the values is unambiguously attributed to in-plane strain[10] caused by the mismatch of the lattice parameters and the thermal expansion coefficients.

Reports on the determination of the complex dielectric function (ε) for c-GaN are scarce,[13] although knowledge of this quantity is essential for the design of optoelectronic devices. Only pseudodielectric functions ($< \varepsilon >$) were reported for the energy range above the gap where features are observed which are correlated to critical points of the band structure[14,15] or to semicore excitations.[16] Fits of the derivatives of $< \varepsilon >$ yielded transition energies; however, the relative peak magnitudes are not well-preserved in comparison to ε.

The progress in determining fundamental optical properties of cubic GaN depends critically on the crystalline and structural quality of the material. Thick, freestanding c-GaN layers obtained by As-mediated growth on GaAs substrates[1] became only recently available. Nanopillars of c-GaN also show a high optical quality.[17] Another approach is the use of 3C-SiC(001)/Si pseudosubstrates.[10] We demonstrated that the phase-purity and crystalline quality of the binary zinc-blende compounds InN,[18] GaN,[19] and AlN[20] can be considerably improved by growing on smooth freestanding 3C-SiC(001) substrates. In contrast to InN[21] and AlN,[22,23] a comprehensive determination and interpretation of optical properties of GaN grown on this substrate has not been reported so far.

Therefore, the focus of this work is to present optical data obtained by different experimental techniques from the band-gap energy and below up to the vacuum ultraviolet. It allows a comparison with theoretical considerations, opening

 ©2012 American Physical Society

access to the electronic band structure of this material. All spectra presented here are recorded from the same high-quality c-GaN layer for comparability. First, we introduce the epitaxial process and the sample; then, after describing the optical techniques, we present data of the excitonic region of c-GaN. We briefly discuss defect-related luminescence features before we finally show the dielectric function up to 20 eV. The data are discussed in detail and compared to theoretical findings.

II. EXPERIMENTAL

The sample under study is a high-quality zinc-blende GaN(001) film grown by plasma-assisted molecular beam epitaxy on a freestanding 3C-SiC(001) substrate.[2,19] Prior to growth, the SiC substrate was cleaned by organic solvents and a buffered oxide etch, followed by an annealing step at 500 °C for 10 h. The growth started with a c-GaN nucleation layer of about 8 nm thickness deposited at 600 °C followed by 616 nm of c-GaN grown at 720 °C. Absorption and desorption of gallium layers on the sample's surface were monitored by reflectivity of high-energy electron diffraction, allowing for a precise control of the growth process and yielding a very smooth surface. Atomic force microscopy revealed a root-mean-square roughness of 1.2 nm of the film, which was confirmed by ellipsometry.

The concentration of donors in the layer was estimated by C-V measurements to be $N_D = 2 \times 10^{17}$ cm^{-3}, assuming a vanishing compensating acceptor density and full activation of presumably shallow donors. As a first attempt, this assumption has also been common practice, e.g., in unintentionally n-type wurtzite GaN as an analogous case. High-resolution x-ray diffractometry yielded nearly identical in-plane ($a_\parallel =$ 4.507 Å) and out-of-plane ($a_\perp = 4.505$ Å) lattice parameters. In contrast to earlier reports on c-GaN, we have determined the lattice parameter $a_\parallel$ by grazing incidence in-plane diffraction, yielding a value specifically valid for the near-surface region which is under optical investigation. If any remaining residual strain is present in our sample, it would be very small and of biaxial tensile type ($|\epsilon| < 5 \times 10^{-4}$). The full width at half maximum (FWHM) of the x-ray diffraction ω scan amounts to 25 arcmin for the GaN(002) reflex, which is expected for the thickness of the film.[24]

To uncover the optical properties around the band edge of c-GaN, standard photoluminescence (PL), PR, and photoluminescence excitation (PLE) spectroscopy were performed. For these experiments, the sample was placed in a variable-temperature cryostat cooled by liquid helium. A HeCd laser ($\lambda = 325$ nm) was exciting the sample for PL and PR, while the monochromatic probe light for PR and the excitation for PLE was provided by a 100 W Xe lamp dispersed by a grating monochromator. The spectral resolution was for all techniques better than 1 meV at 3.3 eV. Additionally, spectroscopic ellipsometry at two different setups was employed. At room temperature, a variable-angle ellipsometer (J.A. Woollam) between 1 and 6.4 eV was used at three different angles of incidence (60°, 67°, and 74°). For data up to 20 eV, we accessed the dedicated rotating analyzer ellipsometer attached to the Berlin electron storage ring for synchrotron radiation (BESSY II). This setup also allows for cooling the sample down to $T = 10$ K by a cold-finger sample holder cooled again by liquid helium. The angle of incidence is there fixed to 67.5° below and to 45° above 10 eV. Details about the setup at BESSY II can be found elsewhere.[15] For the present work, a spectral resolution of 1 meV at 3.3 eV decreasing to 5 meV at 15 eV was used. The ellipsometric parameters Ψ and Δ from both setups were first merged and then fitted by a sophisticated multilayer model,[25] allowing the extraction of the complex dielectric function of c-GaN. Besides the different materials and the layer thicknesses, interface and surface roughness were also fully taken into account.

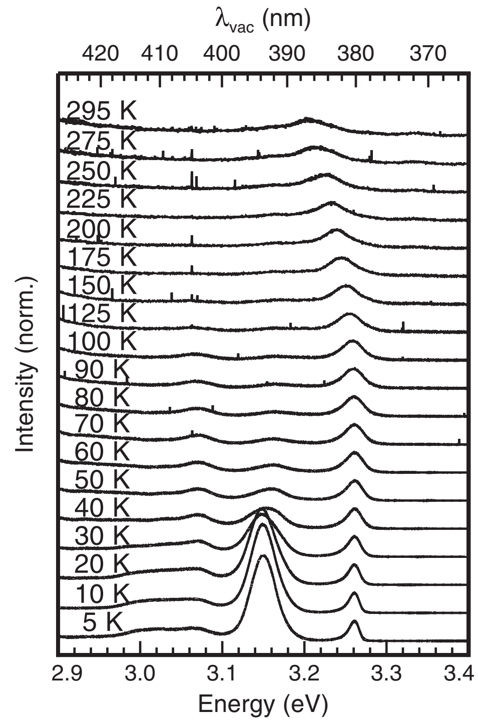

FIG. 1. Temperature-dependent photoluminescence spectra around the band edge. The spectra are normalized to the exciton band and shifted vertically for clarity.

III. RESULTS AND DISCUSSION

A. Band-gap region

Temperature-dependent PL spectra are presented in Fig. 1. The spectra are dominated by several c-GaN near-band-edge recombinations. At $T = 5$ K only a very weak and unstructured band at 3.466 eV related to small wurtzite inclusions is found (not shown here). However, its integrated intensity is a factor of ≈60 weaker than that of the 3.261 eV band of c-GaN alone, corroborating the outstanding material purity.

The band at around 3.261 eV can be followed up to room temperature and is assigned to overlapping-bound and free-exciton recombinations, in agreement with earlier reports.[17,26,27] The FWHM of this band at 5 K is 14.7 meV, a reasonably low value for c-GaN.[28] For increasing temperature, a slight blueshift of the emission maximum can be found, which is interpreted as thermal dissociation of donor bound

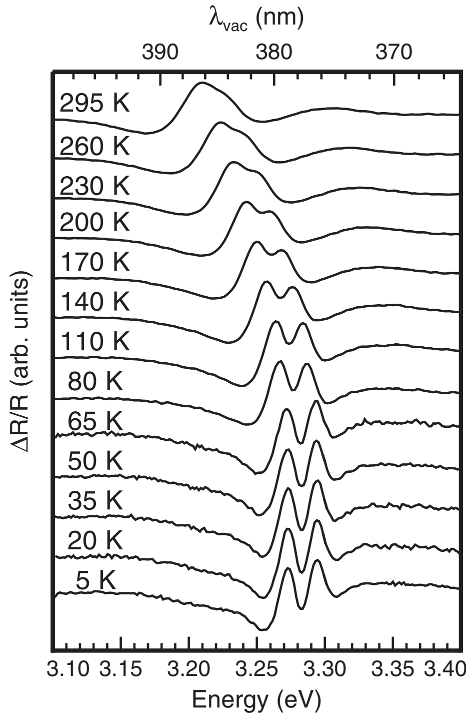

FIG. 2. Photoreflectance spectra measured at different temperatures. The spectra are vertically shifted for clarity.

excitons, before the emission redshifts parallel to the decrease of the band-gap energy of c-GaN.

As an independent proof of the interpretation for the excitonic part of the PL spectra, temperature-dependent PR was measured. The results are presented in Fig. 2 and show two distinct resonances which are identified as free exciton contributions. We fit the PR line shape around the absorption edge by the model developed by Aspnes:[29]

$$\frac{\Delta R}{R}(\hbar\omega) = \Re \sum_j \left(\frac{A_j e^{i\phi_j}}{(\hbar\omega - E_j + i\Gamma_j)^{m_j}} \right), \quad (1)$$

where A_j is the amplitude and ϕ_j the phase of the spectrum, respectively. The energy position and broadening of a transition are represented by E_j and Γ_j. The exponent m_j equals 2 for the first derivative of discrete excitons, and the third derivative contribution from the broadened exciton continuum of three-dimensional M_0 critical points is modeled by $m_j = 2.5$.[29] Representative fits for characteristic temperatures of $T = 5$, 80, and 295 K are presented in Fig. 3.

This procedure yields the exact transition energies of these excitons again as a function of temperature.[10] A comparison of the PL exciton peak energies and the PR transition energies is shown in Fig. 4. As expected, the PL peak overlaps with the lower exciton transition from PR at elevated temperatures, while at $T = 5$ K the difference between PL (3.261 eV) and PR (3.271 eV) is 10 meV, being identical to the binding energy of the free exciton at the neutral donor, the

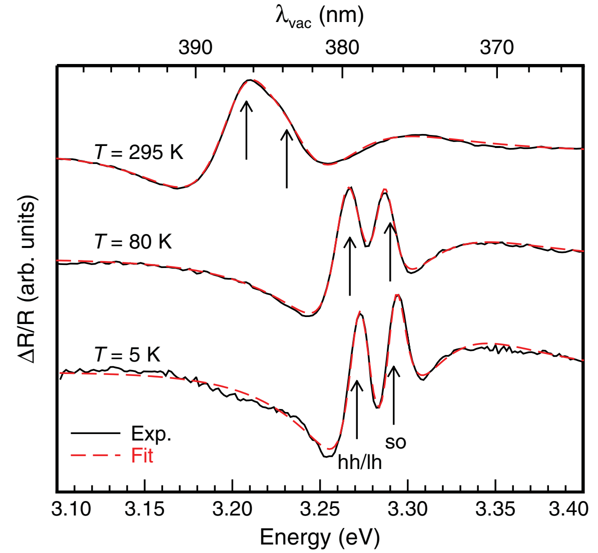

FIG. 3. (Color online) Photoreflectance spectra (continuous lines) at 5, 80, and 295 K and their corresponding line-shape fits (dashed red curves). The characteristic energy positions from the fits are marked by vertical arrows.

localization energy. Similar values were again reported by other groups before.[17,28,30] At temperatures higher than about 120 K, the difference in PL peak and free exciton transition nearly vanishes. This is understandable, as the localization energy of the bound excitons (10 meV) equals $k_B T$ at around 120 K (10.3 meV); thus bound excitons are no longer stable at temperatures above 120 K.

In PR we observe only two excitonic contributions, despite the fact that we deal with three valence bands: the heavy hole (hh), light hole (lh), and the split-off (so) bands. However, the hh and lh bands are degenerate for strain-free material what is mirrored by the nearly identical in-plane and out-of-plane lattice parameters. The complete degeneracy of the lh and hh valence bands is also corroborated by the fact that the hh/lh exciton transitions in PR show the same broadening factor of $\Gamma = 10$ meV at 5 K as the so exciton.[31] The energy distance

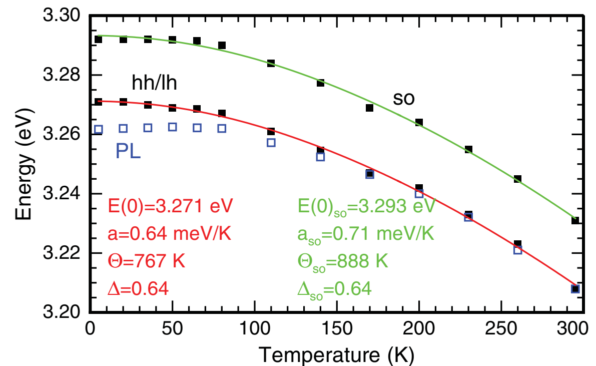

FIG. 4. (Color online) Transition energies obtained by photoreflectance line-shape fits (filled squares) and photoluminescence peak energies (open squares) as a function of temperature. The red and green continuous curves are a fit using the model of Pässler with the parameters shown in the figure as described in the text.

between *hh*/*lh* and *so* excitons is found to be 21 ± 1 meV. Now the temperature dependence of the excitons can be perfectly fitted by the semiempirical model introduced by Pässler[32] (Fig. 4):

$$E(T) = E(0) - a\Theta\left\{\frac{1-3\Delta^2}{e^{\Theta/T}-1} + \frac{3\Delta^2}{2}\left[\sqrt[6]{1+\frac{\pi^2}{3+3\Delta^2}\left(\frac{2T}{\Theta}\right)^2 + \frac{3\Delta^2-1}{4}\left(\frac{2T}{\Theta}\right)^3 + \frac{8}{3}\left(\frac{2T}{\Theta}\right)^4 + \left(\frac{2T}{\Theta}\right)^6} - 1\right]\right\}. \quad (2)$$

We thus report the parameters $E(0) = 3.271$ eV, $a = 0.64$ meV/K, $\Theta = 767$ K, and $\Delta = 0.64$ for the *hh*/*lh* excitons, and $E(0) = 3.293$ eV, $a = 0.71$ meV/K, $\Theta = 888$ K, and $\Delta = 0.64$ for the *so* excitons.

At lower energies in PL (Fig. 1), several additional luminescence contributions are observed centered at 3.147 eV, and weaker bands around 3.056 and 3.010 eV in the 5 K spectrum. The latter one is very weak and already completely untraceable in spectra at $T = 40$ K and above. The other two bands are separated by ≈91 meV, close to the longitudinal phonon energy in wurtzite, and in zinc-blende GaN,[33] we interpret the band around 3.056 eV, therefore, as a LO phonon replica of the 3.147 eV contribution. This band exhibits the typical characteristics of a donor-acceptor pair (DAP) transition, seemingly blueshifting with increasing temperature. It quenches at the expense of a closely related higher energy transition which can be therefore identified as free-to-bound transition, in our case most likely an electron-to-acceptor (e^-A^0) band. A line-shape analysis of DAP and (e^-A^0) bands allows some further insight into the participating defect states. Using a band gap of $E_G = 3.295$ eV at 5 K, as substantiated below, the acceptor binding energy amounts to $E_A = 130 \pm 5$ meV. The more abundant contaminating atoms are, however, the donors, whose binding energy can finally be calculated thanks to their known density using[34]

$$E_D = E_G - E_{DAP} - E_A + \frac{e^2}{4\pi\varepsilon\langle r\rangle}. \quad (3)$$

Here, E_{DAP} is the peak energy of the DAP, and E_D and E_A are donor and acceptor binding energies, respectively. e is the elementary charge, $\varepsilon = \varepsilon_0\varepsilon_s$ the dielectric constant given by the permittivity of vacuum ε_0 and the static dielectric constant $\varepsilon_s = 9.44$ (see below), and $\langle r\rangle = (3/4\pi N_D)^{1/3}$ the average donor-acceptor pair separation. We obtain $E_D = 30$ meV for c-GaN, a value very close to donor binding energies of the common trace impurities silicon and oxygen in wurtzite GaN.[35] With the natural assumption that the donor bound exciton centered at 3.261 eV at 5 K is identical to the donor participating in the DAP recombination and the knowledge of the free exciton resonance, we attribute the exciton localization energy of 10 meV to the donor with $E_D = 30$ meV in c-GaN.

The exciton transition energies extracted from PR and PL are of high precision, which is illustrated by comparing results from our different measurement techniques; in Fig. 5 a comparison at low temperature is shown. We find again the near-band-gap excitonic transition in PL being composed of donor bound excitons dominating at this temperature and a very weak contribution from the free *hh*/*lh* exciton at its high-energy wing, in agreement with our previous analysis. In contrast, in PLE and the imaginary part of the dielectric function ε_2 no signature of discrete excitonic resonances are detected. We attribute this to the different measurement techniques and the occurrence of a strong surface field in c-GaN. Both PLE and ellipsometry mirror the optical properties within the light absorption depth which amounts for c-GaN ≈100 nm around the band gap (the inverse of the absorption

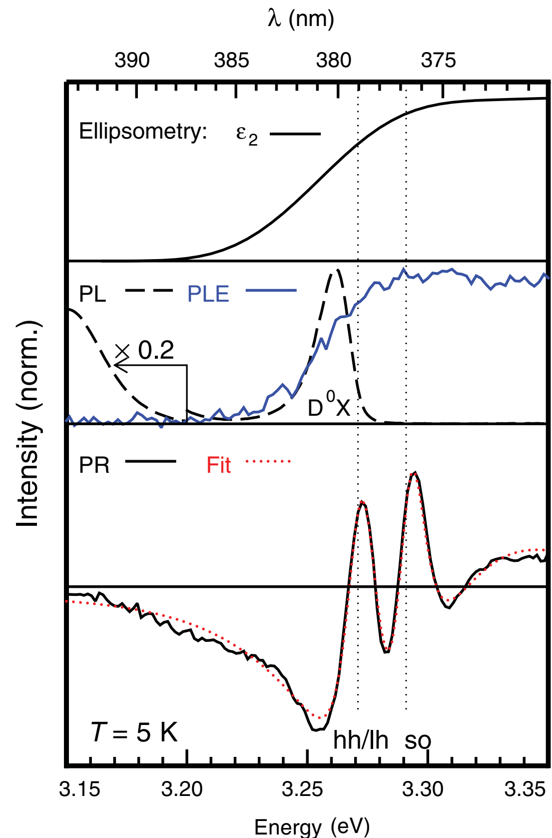

FIG. 5. (Color online) Comparison of results obtained by four optical techniques at low temperature around the band edge. At the bottom, photoreflectance (black continuous line) and the overlayed corresponding fit (dotted) are shown. In the center, photoluminescence and photoluminescence excitation (monitored at around 3.15 eV) are shown, and at the top, the imaginary part of the dielectric function ε_2 is presented. Vertical dotted lines mark the energy positions of the two excitons from the line-shape fit to the photoreflectance spectrum.

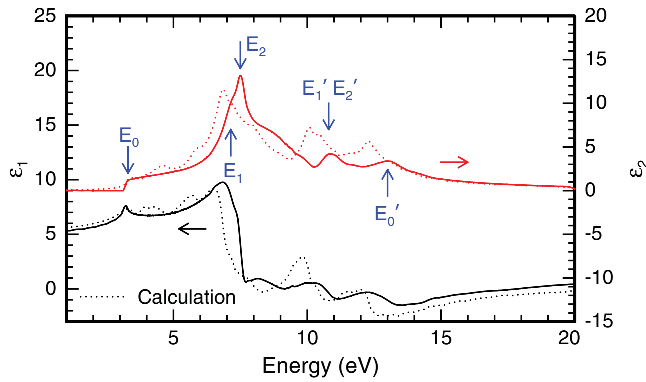

FIG. 6. (Color online) Real (ε_1) and imaginary (ε_2) parts of the dielectric function of c-GaN from 1 to 20 eV. Experimental data recorded at 295 K (continuous curves) are compared to theoretical calculations (dotted traces) reported in Ref. 43.

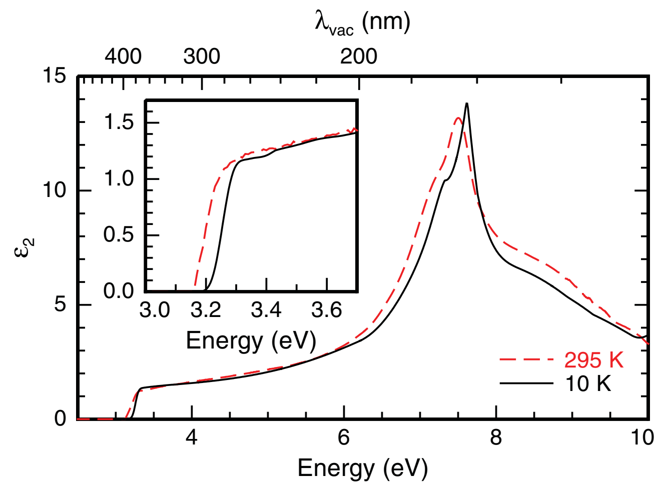

FIG. 7. (Color online) Comparison of the imaginary part (ε_2) of the dielectric function at 295 K (red dashed curve) and 10 K (continuous black curve) up to 10 eV. The inset shows an enlargement of the band-gap region.

coefficient obtained from the dielectric function as described in Ref. 25). In Ref. 36 a surface Fermi-level pinning of 0.4 eV in c-GaN was found. Combining this value with the known donor density $N_D = 2 \times 10^{17}$ cm^{-3} of our sample, we have a surface field of around 175 kV/cm present and a depletion depth of 92 nm. This field strength is about twice the ionization field strength for excitons in GaN of around 90 kV/cm,[37] therefore prohibiting their observance. Only by optical methods like PL or PR, where an intense high-energy laser beam is directed onto the sample, can this surface field be screened, leading to visible excitons in such methods.

In the literature, the free exciton binding energy E_{bX} in c-GaN is reported to be similar to the one in wurtzite GaN. Values of 22 meV,[38] 25 meV,[30] and 26 meV[39] are estimated. As the Luttinger parameters for c-GaN are not known yet, we use recent theoretical effective mass values for c-GaN[40] to estimate reduced effective masses of $\mu_{hh/lh} = 0.15m_0$ and $\mu_{so} = 0.12m_0$. In a simple hydrogen model ($E_{bX} = 13.6\,\text{eV}\frac{\mu}{m_0\varepsilon_s^2}$ with $\varepsilon_s = 9.44$ from Sec. III C), exciton binding energies of 24 meV for the *hh*/*lh* excitons and 18 meV for the *so* excitons are obtained. The band gap of c-GaN is thus $E_0 = 3.295$ eV ($T = 5$ K), and Δ_{so} is found to be 15 meV from the exciton splitting of 21 meV reduced by the difference of the exciton binding energies. In the literature, reports on Δ_{so} of c-GaN are sparse. Renard *et al.* have reported a value of 16.8 meV (Ref. 17) and Ramírez-Flores and co-workers 17 meV.[41] For comparison, density functional theory yields a value of $\Delta_{so} = 20.2$ meV.[40]

B. High-energy transitions

In Fig. 6 the complete dielectric function of c-GaN is shown in an energy range between 1 and 20 eV measured at $T = 295$ K. This is a significant step forward compared to Ref. 15, where only a pseudodielectric function was presented, or to Ref. 42, showing only the energy region up to 10 eV. The imaginary part of the dielectric function ε_2 represents the absorption of c-GaN. The direct band gap E_0 is found as the onset of ε_2 at ≈3.2 eV, in agreement with our preceding discussion. Higher critical points are seen as pronounced features in ε_2. After careful comparison with earlier results and calculated band structures of c-GaN[15,40,42,43] and in analogy to the corresponding case of c-AlN both experimentally[22] and theoretically,[23] we can assign some of the more prominent peaks of ε_2. The shoulder at around 7.23 eV (E_1) is identified to stem from interband transitions in the region of the L point. E_2 clearly peaking at 7.51 eV is assigned to X-point absorption, where the conduction and valence band levels are more parallel for a larger part of the Brillouin zone, thus leading to a sharp feature in the dielectric function. At even higher energy, at 10.72 eV, we detect the spectrally overlapping E_1' and E_2' transitions. Their spectral coincidence in c-GaN becomes especially clear when their position is traced as a function of aluminum concentration in zinc-blende aluminum gallium nitride alloys.[44] E_1' and E_2' are absorption contributions of photons from the uppermost valence band to the next higher conduction bands at the L and X points, respectively. The same transition at the Γ point of the Brillouin zone is labeled E_0' and detected at 12.87 eV. The spin-orbit splittings of the valence bands are not resolvable here, as Δ_{so} is calculated to amount to less than 40 meV for the Γ and L points.[40] Inspection of a calculated dielectric function (also shown in Fig. 6), which was already published in 1999,[43] shows a similar line shape, further confirming our assignments. However, the calculated dielectric function was shifted arbitrarily to match the band-gap value of c-GaN, as no quasiparticle corrections have been applied in these early computations. Therefore, it is expected that the spectral weights of the theoretical curve have to be slightly redistributed to lower energies, which would allow an even better assignment of critical points to features in ε_2.[23]

The dielectric function of c-GaN was also measured at $T = 10$ K up to an energy of 10 eV, as higher energies were not accessible with an inserted cryostat. The comparison of the imaginary part of the dielectric function ε_2 for both temperatures is presented in Fig. 7. We find sharper features at lower temperatures and an overall blueshift of the dielectric function. The decreasing linewidth and increasing amplitude

TABLE I. Measured and calculated[40] optical transition energies E_i and E_i' from the highest valence to the first two conduction bands at high-symmetry points of the Brillouin zone for c-GaN. All values are in electronvolts.

	Theory ($T = 0$ K)					Experiment		
	E_{vb}	E_{cb}	E_{cb}'	E_i	E_i'	E_i (10 K)	E_i (295 K)	E_i' (295 K)
Γ ($i = 0$)	0	3.427	12.401	3.427	12.401	3.295	3.232	12.87
L ($i = 1$)	−1.107	6.600	10.811	7.707	11.918	7.33	7.23	10.72
X ($i = 2$)	−3.052	4.703	8.716	7.755	11.768	7.62	7.51	10.72

of, e.g., E_2 is an indication of the mainly phononic origin of the broadening instead of sample-quality-dependent inhomogeneous broadening. This shows independently the high optical quality of our c-GaN layer. The shift of the absorption onset at the band gap due to temperature amounts again to about 63 meV (best seen in the inset of Fig. 7), in agreement with our above analysis. The high-energy critical points E_1 and E_2 shift by 0.1 and 0.11 eV due to the temperature decrease, respectively. A larger shift of higher critical points as a function of temperature as compared to the band gap is also known from different material systems, e.g., AlGaAs.[45]

Finally, both ε_2 spectra in Fig. 6 exhibit a shoulder between 8.5 and 9 eV. Based on the band-structure calculations presented in Ref. 40 it can be tentatively assigned to transitions around the K point of the Brillouin zone. For a comparison of the experimental transition energies with the results of the band-structure calculations, one has to keep in mind that the theoretical data depend critically on both the used exchange and correlation (XC) potential and the quasiparticle corrections to overcome the density functional band-gap problem.[6,40] A recent comparison[40] demonstrated that the AM05 XC functional yields for the c-GaN lattice parameter $a = 4.495$ Å, which is only slightly lower than the experimental value. Then, a quasiparticle gap of 3.427 eV is obtained by self-energy corrections within the HSE + G_0W_0 (Heyd, Scuseria, and Ernzerhof functional plus Greens-function and dynamically screened Coulomb interaction) approach. The method yields energies of the uppermost valence band E_{vb} and the first two conduction bands E_{cb} and E_{cb}' at the high-symmetry points Γ, L, and X, which are summarized in Table I. The corresponding interband transition energies E_1, E_2, and E_0' are in very good agreement with the experiment, and deviations up to 1.2 eV are found for E_1' and E_2'. The behavior at the X point becomes particularly important when studying cubic AlGaN alloys.[46] The current studies emphasize a value between 4.57 and 4.7 eV for E_{cb}, which is consistent with the previously reported value of 4.65 eV.[46]

C. Below band-gap dispersion

The dispersive below-gap region in ε_1 is equal to the square of the refractive index (as long as $\varepsilon_2 = 0$) and thus is of special interest for the design of optoelectronic devices. This dispersion can be modeled by the analytic expression:[47]

$$\varepsilon_1(\hbar\omega) = 1 + \frac{2}{\pi}\left(\frac{A_G}{2}\ln\frac{E_H^2 - (\hbar\omega)^2}{E_G^2 - (\hbar\omega)^2} + \frac{A_H E_H}{E_H^2 - (\hbar\omega)^2}\right). \quad (4)$$

Here, E_G and E_H represent average energies of the band gap and the higher energy contributions, respectively. The amplitudes A_G and A_H weight these accordingly. In the case of c-GaN, we obtain $E_G = 3.23$ eV, $E_H = 8.65$ eV, $A_G = 1.55$, and $A_H = 45.29$. The high-energy limit ($\hbar\omega \to 0$) of ε_1 is known as high-frequency dielectric constant ε_∞ and is found to be 5.31 for c-GaN. The static dielectric constant can be obtained via the Lyddane-Sachs-Teller relation $\varepsilon_s = (\omega_{LO}/\omega_{TO})^2\varepsilon_\infty = 9.44$ with the longitudinal and transversal optical phonon frequencies $\omega_{LO} = 740$ cm^{-1} and $\omega_{TO} = 555$ cm^{-1},[48] respectively. Our results for $\varepsilon_1(\hbar\omega)$ are in good agreement with earlier reports focusing on the analysis of the dielectric function in the energy range below 5 eV.[13]

IV. SUMMARY

In conclusion, we have studied a high-quality nearly unstrained zinc-blende GaN epitaxial layer grown on 3C-SiC by optical methods. We have shown comprehensive spectra by different techniques of the near-band-gap excitonic region. The degenerate light and heavy hole exciton transition is found to be located at 3.271 eV at 5 K and at 3.208 eV at 295 K, respectively. It was found that $\Delta_{so} \approx 15$ meV. Furthermore, the complex dielectric function has been presented in an energy range from 1 up to 20 eV, and certain prominent features have been assigned to distinct interband transitions in the Brillouin zone. Finally, we have modeled the dispersion of ε_1 in the below-band-gap region and presented an analytical expression. We obtain $\varepsilon_\infty = 5.31$ and $\varepsilon_s = 9.44$ for c-GaN.

ACKNOWLEDGMENTS

This work was supported financially by the HZB, the European Commission within the Seventh Framework Program (NanoCharM), and the DFG graduate program "Micro- and Nanostructures in Optoelectronics and Photonics" and Project No. As 107/4-1. D.J.A. wants to thank Dr. H. Nagasawa at HOYA Corporation for the supply of the excellent 3C-SiC substrates.

*martin.feneberg@ovgu.de
†Present address: I. Physikalisches Institut, Justus-Liebig-Universität Giessen, Heinrich-Buff-Ring 16, 35392 Giessen, Germany.

[1] S. V. Novikov, N. M. Stanton, R. P. Campion, R. D. Morris, H. L. Geen, C. T. Foxon, and A. J. Kent, Semicond. Sci. Technol. **23**, 015018 (2008).

[2]D. J. As, Microelectron. J. **40**, 204 (2009).
[3]O. Ambacher and V. Cimalla, in *Polarization Effects in Semiconductors: From Ab Initio Theory to Device Applications*, edited by C. Wood and D. Jena (Springer, New York, 2008), p. 27.
[4]E. A. DeCuir Jr., M. O. Manasreh, E. Tschumak, J. Schörmann, D. J. As, and K. Lischka, Appl. Phys. Lett. **92**, 201910 (2008).
[5]H. Machhadani, M. Tchernycheva, S. Sakr, L. Rigutti, R. Colombelli, E. Warde, C. Mietze, D. J. As, and F. H. Julien, Phys. Rev. B **83**, 075313 (2011).
[6]C. Mietze, M. Landmann, E. Rauls, H. Machhadani, S. Sakr, M. Tchernycheva, F. H. Julien, W. G. Schmidt, K. Lischka, and D. J. As, Phys. Rev. B **83**, 195301 (2011).
[7]D. Lagarde, A. Balocchi, H. Carrère, P. Renucci, T. Amand, X. Marie, S. Founta, and H. Mariette, Phys. Rev. B **77**, 041304 (2008).
[8]N. Zainal, S. V. Novikov, C. J. Mellor, C. T. Foxon, and A. J. Kent, Appl. Phys. Lett. **97**, 112102 (2010).
[9]K. W. Edmonds, S. V. Novikov, M. Sawicki, R. P. Campion, C. R. Staddon, A. D. Giddings, L. X. Zhao, K. Y. Wang, T. Dietl, C. T. Foxon, and B. L. Gallagher, Appl. Phys. Lett. **86**, 152114 (2005).
[10]A. Philippe, C. Bru-Chevallier, H. Gamez-Cuatzin, G. Guillot, E. Martinez-Guerrero, G. Feuillet, B. Daudin, P. Aboughé-Nzé, and Y. Monteil, Phys. Status Solidi B **216**, 247 (1999).
[11]R. Goldhahn, J. Scheiner, S. Shokhovets, T. Frey, U. Köhler, D. J. As, and K. Lischka, Appl. Phys. Lett. **76**, 291 (2000).
[12]D. J. As, T. Frey, D. Schikora, K. Lischka, V. Cimalla, J. Pezoldt, R. Goldhahn, S. Kaiser, and W. Gebhardt, Appl. Phys. Lett. **76**, 1686 (2000).
[13]U. Köhler, D. J. As, B. Schöttker, T. Frey, K. Lischka, J. Scheiner, S. Shokhovets, and R. Goldhahn, J. Appl. Phys. **85**, 404 (1999).
[14]A. Kasic, M. Schubert, T. Frey, U. Köhler, D. J. As, and C. M. Herzinger, Phys. Rev. B **65**, 184302 (2002).
[15]C. Cobet, R. Goldhahn, W. Richter, and N. Esser, Phys. Status Solidi B **246**, 1440 (2009).
[16]M. Rakel, C. Cobet, N. Esser, F. Fuchs, F. Bechstedt, R. Goldhahn, W. G. Schmidt, and W. Schaff, Phys. Rev. B **77**, 115120 (2008).
[17]J. Renard, G. Tourbot, D. Sam-Giao, C. Bougerol, B. Daudin, and B. Gayral, Appl. Phys. Lett. **97**, 081910 (2010).
[18]J. Schörmann, D. J. As, K. Lischka, P. Schley, R. Goldhahn, S. F. Li, W. Löffler, M. Hetterich, and H. Kalt, Appl. Phys. Lett. **89**, 261903 (2006).
[19]J. Schörmann, S. Potthast, D. J. As, and K. Lischka, Appl. Phys. Lett. **90**, 041918 (2007).
[20]T. Schupp, G. Rossbach, P. Schley, R. Goldhahn, M. Röppischer, N. Esser, C. Cobet, K. Lischka, and D. J. As, Phys. Status Solidi A **207**, 1365 (2010).
[21]P. Schley, R. Goldhahn, C. Napierala, G. Gobsch, J. Schörmann, D. J. As, K. Lischka, M. Feneberg, and K. Thonke, Semicond. Sci. Technol. **23**, 055001 (2008).
[22]M. Röppischer, R. Goldhahn, G. Rossbach, P. Schley, C. Cobet, N. Esser, T. Schupp, K. Lischka, and D. J. As, J. Appl. Phys. **106**, 076104 (2009).
[23]A. Riefer, F. Fuchs, C. Rödl, A. Schleife, F. Bechstedt, and R. Goldhahn, Phys. Rev. B **84**, 075218 (2011).
[24]D. J. As, Proc. SPIE **7608**, 76080G-1 (2010).
[25]R. Goldhahn, Acta Phys. Polonica A **104**, 123 (2003).
[26]H. Okumura, S. Misawa, and S. Yoshida, Appl. Phys. Lett. **59**, 1058 (1991).
[27]S. Strite, J. Ruan, Z. Li, N. Manning, A. Salvador, H. Chen, D. J. Smith, W. J. Choyke, and H. Morkoç, J. Vac. Sci. Technol. B **9**, 1924 (1991).
[28]H. Yaguchi, J. Wu, B. Zhang, Y. Segawa, H. Nagasawa, K. Onabe, and Y. Shiraki, J. Cryst. Growth **195**, 323 (1998).
[29]D. E. Aspnes, Surf. Sci. **37**, 418 (1973).
[30]J. Menniger, U. Jahn, O. Brandt, H. Yang, and K. Ploog, Phys. Rev. B **53**, 1881 (1996).
[31]C. Bru-Chevallier, S. Fanget, A. Philippe, C. Dubois, E. Martinez-Guerrero, B. Daudin, P. Aboughé-Nzé, and Y. Monteil, Phys. Status Solidi A **183**, 67 (2001).
[32]R. Pässler, Phys. Rev. B **66**, 085201 (2002).
[33]J. Ibáñez, S. Hernández, E. Alarcón-Lladó, R. Cuscó, L. Artús, S. V. Novikov, C. T. Foxon, and E. Calleja, J. Appl. Phys. **104**, 033544 (2008).
[34]P. Y. Yu and M. Cardona, *Fundamentals of Semiconductor Physics and Materials Properties*, 4th ed. (Springer, Berlin, 2010), p. 356.
[35]W. J. Moore, J. A. Freitas, G. C. B. Braga, R. J. Molnar, S. K. Lee, K. Y. Lee, and I. J. Song, Appl. Phys. Lett. **79**, 2570 (2001).
[36]R. Kudrawiec, E. Tschumak, J. Misiewicz, and D. J. As, Appl. Phys. Lett. **96**, 241906 (2010).
[37]A. T. Winzer, G. Gobsch, R. Goldhahn, D. Fuhrmann, A. Hangleiter, A. Dadgar, and A. Krost, Phys. Rev. B **74**, 125207 (2006).
[38]Z. X. Liu, A. R. Goñi, K. Syassen, H. Siegle, C. Thomsen, B. Schöttker, D. J. As, and D. Schikora, J. Appl. Phys. **86**, 929 (1999).
[39]S. Shokhovets, G. Gobsch, and O. Ambacher, Phys. Rev. B **74**, 155209 (2006).
[40]L. C. de Carvalho, A. Schleife, and F. Bechstedt, Phys. Rev. B **84**, 195105 (2011).
[41]G. Ramírez-Flores, H. Navarro-Contreras, A. Lastras-Martinez, R. C. Powell, and J. E. Greene, Phys. Rev. B **50**, 8433 (1994).
[42]S. Logothetidis, J. Petalas, M. Cardona, and T. D. Moustakas, Phys. Rev. B **50**, 18017 (1994).
[43]L. X. Benedict and E. L. Shirley, Phys. Rev. B **59**, 5441 (1999).
[44]M. Röppischer, PhD Thesis, Berlin (2011).
[45]S. Logothetidis, M. Cardona, and M. Garriga, Phys. Rev. B **43**, 11950 (1991).
[46]F. Sökeland, M. Rohlfing, P. Krüger, and J. Pollmann, Phys. Rev. B **68**, 075203 (2003).
[47]S. Shokhovets, R. Goldhahn, G. Gobsch, S. Piekh, R. Lantier, A. Rizzi, V. Lebedev, and W. Richter, J. Appl. Phys. **94**, 307 (2003).
[48]E. Alarcón-Lladó, J. Ibáñez, R. Cuscó, L. Artús, S. V. Novikov, and C. T. Foxon, Semicond. Sci. Technol. **24**, 115019 (2009).